Accuracy of the Parallel-Plate Analogy for Representation of Viscous Flow Between Coaxial Cylinders

R. A. WORTH, *Department of Polymer and Fibre Science, The University of Manchester Institute of Science and Technology, Manchester, M60 1QD, England*

Synopsis

The accuracy of the parallel-plate approximation to represent various viscous flows of non-Newtonian fluids between coaxial cylinders is investigated. Four types of flow are considered: tangential drag flow, tangential pressure flow, axial drag flow, and axial pressure flow. The solutions for flow between parallel plates are compared with the exact solutions, and the errors are plotted against radius ratio for a number of values of the power-law index to provide an indication of the range of usefulness of the parallel-plate analogy.

INTRODUCTION

Because of the complexity of the solutions for viscous flow between coaxial cylinders, it is often necessary to simplify the flow by considering an equivalent parallel-plate geometry, where the width of the plates is equal to the mean circumference of the cylinders, and the plate separation is equal to the difference in the cylinder radii. The parallel-plate analogy is particularly useful where non-Newtonian fluids such as polymer melts are involved. Of considerable importance are (1) tangential flow, when one cylinder rotates relative to the other; (2) tangential flow due to an applied pressure gradient; (3) axial drag flow, when one cylinder moves longitudinally relative to the other; and (4) axial flow due to an applied pressure gradient. Various combinations of these flows may exist. The following examples are encountered in polymer processing: flow through pipe-extrusion dies (type 4), through wire-coating dies (combination of 3 and 4), in the extruder screw channel (type 1), and in spiral molds (type 2).

The accuracy of the parallel-plate analogy depends on the radius ratio of the coaxial cylinders; if the clearance is small compared with the mean radius, the error will be small. However, for relatively large clearances the error involved in using the approximation may be considerable. The four types of flow are analyzed in turn, for both the coaxial-cylinder and parallel-plate geometries, and the accuracy is plotted as a function of radius ratio. It is assumed that the fluid obeys the power-law relationship, and various values of the power-law index are considered. The results give an indication of the degree of confidence with which the parallel-plate approximation may be used for the various flow geometries.

Journal of Applied Polymer Science, Vol. 24, 319–328 (1979)

0021-8995/79/0024-0319$01.00

THEORETICAL

The following assumptions are common to the analyses: the flow is laminar; the flow is isothermal; the flow is time independent; the fluid is incompressible; there is no slip at the fluid boundary; edge or end effects are negligible; and inertia and gravity effects are negligible. In addition, the fluid is assumed to be governed by the power-law equation

$$\tau = \eta \dot{\gamma}^n \tag{1}$$

and the apparent viscosity μ is

$$\mu = \eta \dot{\gamma}^{n-1} \tag{2}$$

Tangential Drag Flow

This type of flow, with the inner cylinder rotating, is illustrated in Fig. 1(A), and the parallel-plate representation is shown in Fig. 1(B).

Coaxial Cylinders

From the momentum equation

$$\frac{1}{r^2}\frac{\partial}{\partial r}(r^2\tau_{r\theta}) = \frac{1}{r}\frac{\partial P}{\partial \theta} = 0 \tag{3}$$

The only nonzero component of the stress tensor is

$$\tau_{r\theta} = \mu r \frac{\partial}{\partial r}\left(\frac{v_\theta}{r}\right) \tag{4}$$

and for a power-law fluid,

$$\tau_{r\theta} = \eta \left[r \frac{\partial}{\partial r}\left(\frac{v_\theta}{r}\right)\right]^n \tag{5}$$

The boundary conditions are $v_\theta = 0$ at $r = R_0$ and $v_\theta = V$ at $r = R_i$. Equations (3) and (5) have been solved[1] to obtain an expression for the flow rate per unit length Q_c in terms of the velocity of the inner cylinder V:

$$Q_c = \frac{VR_i}{2}\left[\beta^2 - 1 - \frac{1}{(1-s)}(\beta^2 - \beta^{2s})\right]/(1 - \beta^{2s}) \tag{6}$$

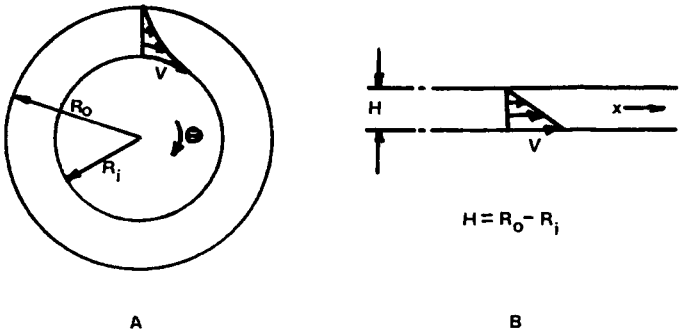

Fig. 1. Tangential drag flow with the inner cylinder rotating for coaxial cylinders (A) and parallel plates (B).

where $s = 1/n$ and $\beta = R_0/R_i$. Equation (6) is not valid for $n = 1$, and the solution for a Newtonian fluid is

$$Q_c = (VR_i/2)(\beta^2 - 1 - 2\beta^2 \log e\beta)/(1 - \beta^2) \tag{7}$$

Analagous expressions may be derived for the case when the outer cylinder rotates by using the boundary conditions $v_\theta = V$ at $r = R_0$ and $v_\theta = 0$ at $r = R_i$.

Parallel Plates

For the equivalent parallel-plate geometry, the velocity gradient is uniform, and the flow rate can be written as

$$Q_p = VH/2 = (V/2)(R_0 - R_i) \tag{8}$$

The quantity ϵ may be defined as follows:

$$\epsilon = Q_p/Q_c \tag{9}$$

ϵ is used as a measure of the accuracy of the parallel-plate representation, values close to unity indicating good accuracy. Curves of ϵ against the radius ratio β are plotted in Fig. 2 for various values of n from 0.2 to 1.0. The accuracy is also plotted for the case when the outer cylinder rotates.

Tangential Pressure Flow

The flow geometry is illustrated in Fig. 3(A), with the equivalent parallel-plate geometry in Fig. 3(B).

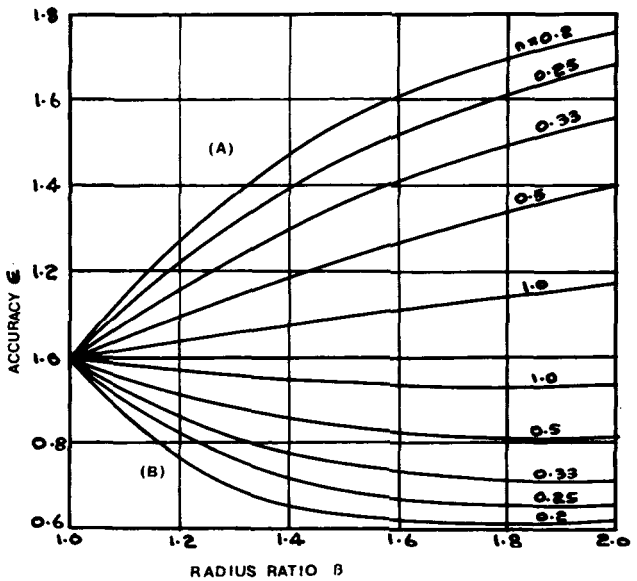

Fig. 2. Accuracy vs radius ratio for tangential drag flow with inner cylinder rotating (A) and outer cylinder rotating (B).

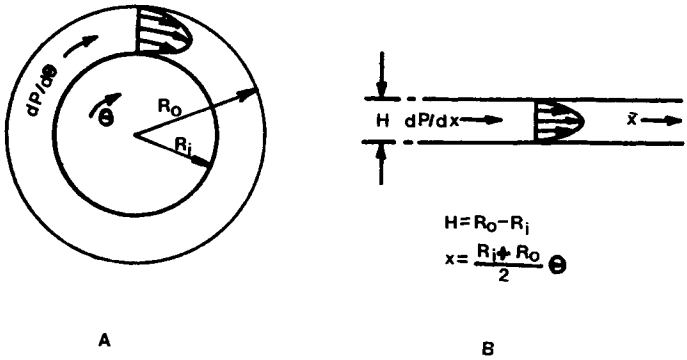

Fig. 3. Tangential pressure flow for coaxial cylinders (A) and parallel plates (B).

Coaxial Cylinders

The momentum equation is

$$\frac{1}{r^2}\frac{\partial}{\partial r}(r^2\tau_{r\theta}) = \frac{1}{r}\frac{\partial P}{\partial \theta} \tag{10}$$

After integrating and rearranging,

$$\tau_{r\theta} = \frac{1}{2}\frac{\partial P}{\partial \theta} + \frac{C_1}{r^2} \tag{11}$$

Again the shear stress is given by eq. 5, and combining eqs. (5) and (11),

$$\frac{\partial}{\partial r}\left(\frac{v_\theta}{r}\right) = \left(\frac{1}{2\eta}\frac{\partial P}{\partial \theta}\right)^s \left(\frac{1}{r^n} + \frac{C_2}{r^{2+n}}\right)^s \tag{12}$$

The velocity profile is obtained by integrating eq. (12);

$$v_\theta = r\left[\left(\frac{1}{2\eta}\frac{\partial P}{\partial \theta}\right)^s \int \left(\frac{1}{r^n} + \frac{C_2}{r^{2+n}}\right)^s dr + C_3\right] \tag{13}$$

and the constants of integration determined from the boundary conditions,

$$v_\theta = 0 \quad \text{at } r = R_i \text{ and } r = R_0$$

The flow rate per unit length is obtained by further integration:

$$Q_c = \int_{R_i}^{R_0} v_\theta dr \tag{14}$$

These equations can only be solved exactly for integer values of s, and for s = 1 (Newtonian fluid) the solution is

$$Q_c = \frac{1}{2\mu}\frac{\partial P}{\partial \theta} R_i^2 \left(\frac{\beta^2 - 1}{4} - \frac{\beta^2}{\beta^2 - 1}(\log e\beta^2)\right) \tag{15}$$

The constant of integration C_2 is related to the coordinate of the plane of zero shear stress (maximum velocity) and must be evaluated numerically for values of s other than unity.

Parallel Plates

For pressure flow between parallel plates, the flow rate per unit length is

$$Q_p = \frac{3n}{2n+1}\frac{H^{(2n+1)/n}}{6}\left(\frac{1}{2\eta}\frac{\partial P}{\partial x}\right)^s \tag{16}$$

where $H = R_0 - R_i$, $x = \theta(R_0 + R_i)/2$, and

$$\frac{\partial P}{\partial x} = \frac{\partial P}{\partial \theta}\left[\tfrac{1}{2}(R_0 + R_i)\right]^{-1}$$

The accuracy ϵ $(=Q_p/Q_c)$ is plotted against β for various values of n in Fig. 4.

Axial Drag Flow

This flow and its parallel-plate representation are illustrated in Fig. 5 for the case when the inner cylinder moves.

Coaxial Cylinders

From the momentum equation,

$$\frac{1}{r}\frac{\partial}{\partial r}(r\tau_{rz}) = \frac{\partial P}{\partial z} = 0 \tag{17}$$

and the stress component for a power law fluid is

$$\tau_{rz} = \eta\left(\frac{\partial v_z}{\partial r}\right)^n \tag{18}$$

The boundary conditions are

$$v_z = V \quad \text{at} \quad r = R_i$$
$$v_z = 0 \quad \text{at} \quad r = R_0$$

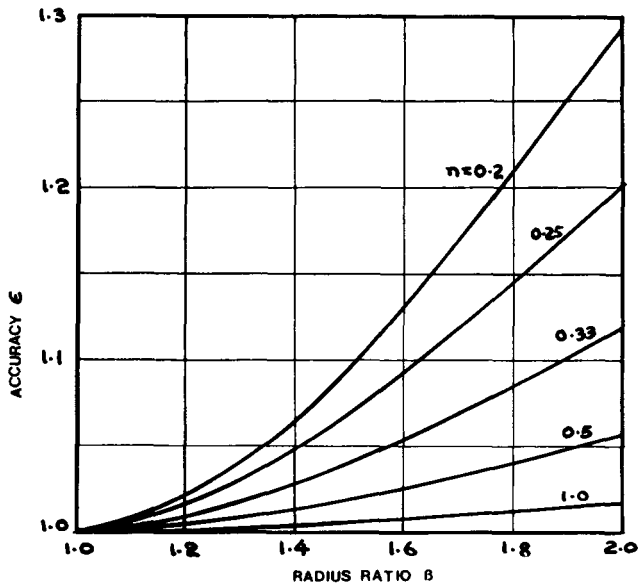

Fig. 4. Accuracy vs radius ratio for tangential pressure flow.

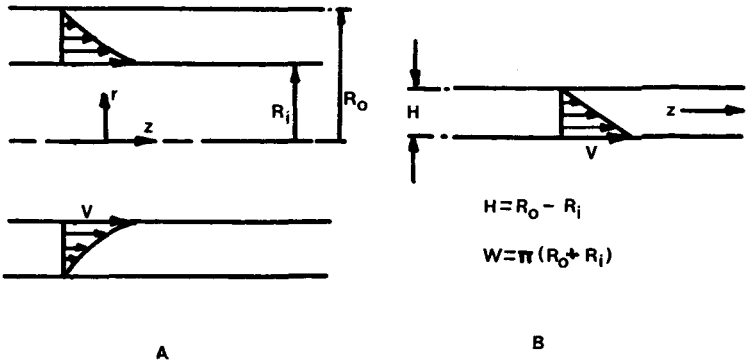

Fig. 5. Axial drag flow with the inner cylinder moving for coaxial cylinders (A) and parallel plates (B).

These equations have been solved[1] to obtain an expression for the flow rate Q_c:

$$Q_c = \frac{\pi V}{2}(R_0^2 - R_i^2)g(\beta,n) \tag{19}$$

where the function $g(\beta,n)$ is defined as

$$g(\beta,n) = \left(\frac{2n-2}{3n-1}\right)\left(\frac{1}{1-\beta^{(1-n)/n}}\right) - \left(\frac{4n}{3n-1}\right)\left(\frac{1}{\beta^2-1}\right) \tag{20}$$

Equation (20) is not valid for $n = 1$, and the correct expression for a Newtonian fluid is

$$g(\beta,1) = \frac{1}{\log e\beta} - \frac{2}{\beta^2-1} \tag{21}$$

Analagous expressions may be obtained for the case when the outer cylinder moves and the inner cylinder is fixed by using the boundary conditions $v_z = 0$ at $r = R_i$ and $v_z = V$ at $r = R_0$.

Parallel Plates

The flow rate is

$$Q_p = WHV/2 \tag{22}$$

where W is the mean circumference, $\pi(R_0 + R_i)$, and $H = R_0 - R_i$. The equation equivalent to eq. (19) is simply

$$Q_p = \frac{\pi V}{2}(R_0^2 - R_i^2) \tag{23}$$

The accuracy ϵ $(=Q_p/Q_c)$ is plotted against β for a number of values of n, for the two cases when either cylinder moves and the other is fixed, in Fig. 6.

Axial Pressure Flow

Pressure flow through an annulus is illustrated in Fig. 7(A), and the parallel-plate representation is shown in Fig. 7(B).

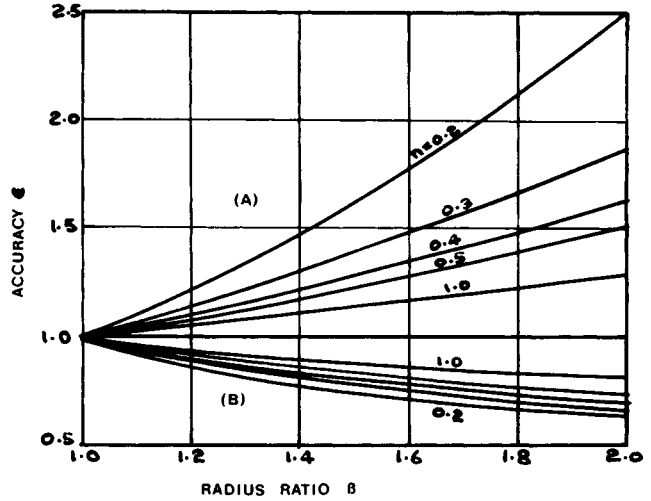

Fig. 6. Accuracy vs radius ratio for axial drag flow for inner cylinder moving (A) and outer cylinder moving (B).

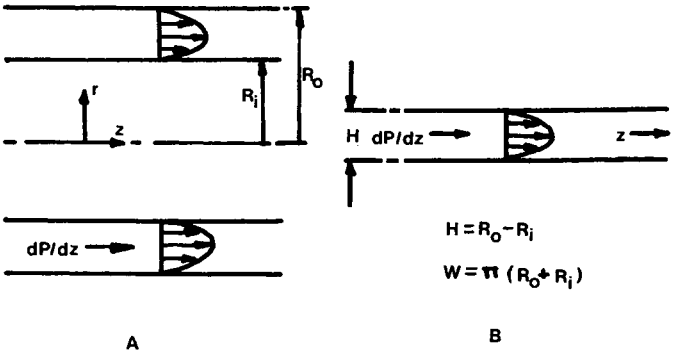

Fig. 7. Axial pressure flow for coaxial cylinders (A) and parallel plates (B).

Coaxial Cylinders

The momentum equation is

$$\frac{1}{r}\frac{\partial}{\partial r}(r\tau_{rz}) = \frac{\partial P}{\partial z} \tag{24}$$

which on integration gives

$$\tau_{rz} = \frac{r}{2}\frac{\partial P}{\partial z} + \frac{C_1}{r} \tag{25}$$

The constant of integration C_1, is related to the coordinate of zero shear stress κR_0. Introducing the condition that $\tau_{rz} = 0$ at $r = \kappa R_0$, eq. (25) becomes

$$\tau_{rz} = \frac{1}{2}\frac{\partial P}{\partial z}\left(r - \frac{(\kappa R_0)^2}{r}\right) \tag{26}$$

The component of the stress tensor is again given by eq. (18), so that

$$\frac{\partial v_z}{\partial r} = \left(\frac{1}{2\eta}\frac{\partial P}{\partial z}\right)^s \left(r - \frac{(\kappa R_0)^2}{r}\right) \tag{27}$$

Fredrickson and Bird[2] integrated the above equation to obtain an expression for the flow rate Q_c. Their solution is of the form

$$Q_c = \pi R_0^{(3n+1)/n} \left(\frac{1}{2\eta}\frac{\partial P}{\partial z}\right)^s \Omega(s,\kappa) \tag{28}$$

The function $\Omega(s,\kappa)$ is given by

$$\Omega(s,\kappa) = \int_\kappa^1 \left|\left(\frac{1}{\beta}\right)^2 - \xi^2\right|^{s+1} \xi^{-s}\, d\xi \tag{29}$$

where ξ is the dimensionless radial coordinate r/R_0. The solution is valid only for integer values of s, and the dimensionless coordinate of zero shear stress κ must be evaluated numerically for values of s other than unity. However, for $R_0 - R_i \ll R_0$, the plane of zero shear stress approaches the midchannel position, i.e., $\kappa \simeq (1 + \beta)/2\beta$.

The solution for a Newtonian fluid is

$$Q_c = \frac{\pi R_0^4}{8\mu}\frac{\partial P}{\partial z}\left[\left(\frac{\beta^4 - 1}{\beta^4}\right) - \left(\frac{\beta^2 - 1}{\beta^2}\right)^2 \left(\frac{1}{\log e\beta}\right)\right] \tag{30}$$

Parallel Plates

The flow rate is

$$Q_p = \frac{3n}{2n+1}\frac{WH^{(2n+1)/n}}{6}\left(\frac{1}{2\eta}\frac{\partial P}{\partial z}\right)^s \tag{31}$$

where $W = \pi(R_0 + R_i)$ and $H = R_0 - R_i$. The accuracy of the parallel-plate approximation, defined as $\epsilon = Q_p/Q_c$, is plotted against β for various values of n in Fig. 8.

CONCLUSIONS

The parallel-plate analogy provides a vast simplification of flow analysis, which results in considerable time saving during the solution of problems, particularly in the case of non-Newtonian flow.[3,4] In fact the exact solution is in some cases intractable without the use of numerical methods. Vaughn and Bergman[4] have commented on this in relation to flow of non-Newtonian fluids (e.g., polymer melts) through annular dies, and their observations are valid for other flow situations. It is important, however, that technologists appreciate that the parallel-plate analogy is an approximation and cannot be used for high values of radius ratio without significant error.

The theoretical curves show that it is valid to use the parallel-plate analogy for values of radius ratio close to unity; however, in general there is a considerable inaccuracy as the radius ratio is increased. The only exception is in the case of pressure flow through an annulus (Figs. 7 and 8), where the accuracy is relatively insensitive to radius ratio. In all cases the error increases as the power-law index n is reduced, i.e., the error is greater for fluids which exhibit a large degree of non-Newtonian (pseudoplastic) behavior.

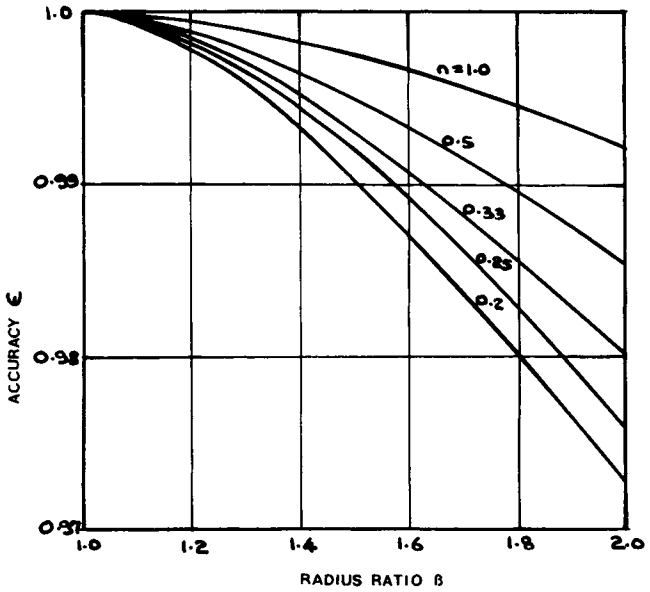

Fig. 8. Accuracy vs radius ratio for axial pressure flow.

Despite the limitations of the parallel-plate approximation, more use may be made of the analogy without loss of accuracy provided that the results are corrected using the curves shown in Figs. 2, 4, 6, and 8.

NOTATION

C	constants of integration
g	function defining flow rate
H	plate separation
n	power-law index
P	pressure
Q_c	flow rate (coaxial cylinders)
Q_p	flow rate (parallel plates)
r	radial coordinate
R_i	inner cylinder radius
R_0	outer cylinder radius
s	$1/n$
v	velocity
V	velocity of inner cylinder
W	width of plates
$x,y,z,$	rectangular coordinate axes
β	radius ratio (R_0/R_i)
$\dot{\gamma}$	shear rate
ϵ	error
η	power-law constant
θ	tangential coordinate
κ	dimensionless coordinate of plane of zero shear stress

μ	viscosity
ξ	dimensionless radial coordinate
τ	shear stress
Ω	function defining flow rate.

References

1. J. M. McKelvey, *Polymer Processing*, Wiley, New York, 1962.
2. A. G. Fredrickson and R. B. Bird, *Ind. Eng. Chem.*, **50,** 347 (1958).
3. J. Parnaby and R. A. Worth, *Proc. Inst. Mech. Eng. London*, **188,** 357 (1974).
4. R. D. Vaughn and P. D. Bergman, *Ind. Eng. Chem., Process Des. Dev.*, **5,** 45 (1966).

Received July 4, 1978